Radio Science

RESEARCH ARTICLE
10.1029/2020RS007105

Special Section:
Beacon Satellite Symposium 2019

Development of an Empirical Model for Estimating the Quiet Day Curve (QDC) Over the Brazilian Sector

S. S. Chen[1], C. M. Denardini[1], L. C. A. Resende[1,2], R. A. J. Chagas[1], J. Moro[2,3], and G. A. S. Picanço[1]

[1]National Institute for Space Research (INPE), São José dos Campos, SP, Brazil, [2]National Space Science Center, Chinese Academy of Science (NSSC/CAS), Beijing, China, [3]Southern Space Coordination (COESU/INPE/MCTI), Santa Maria, RS, Brazil

Key Points:
- An empirical model to estimating the quiet day curve (QDC) is presented
- Fluxgate magnetometer data collected from 12 magnetic stations over South America are used in the model calculation
- The results showed that the values computed by this model are in good agreement with the observational data for the QDC

Correspondence to:
S. S. Chen,
sony.chen@inpe.br

Citation:
Chen, S. S., Denardini, C. M., Resende, L. C. A., Chagas, R. A. J., Moro, J., & Picanço, G. A. S. (2020). Development of an empirical model for estimating the quiet day curve (QDC) over the Brazilian sector. *Radio Science*, *55*, e2020RS007105. https://doi.org/10.1029/2020RS007105

Received 10 MAR 2020
Accepted 20 OCT 2020
Accepted article online 22 OCT 2020

Author Contributions:
Conceptualization: S. S. Chen, C. M. Denardini, L. C. A. Resende, R. A. J. Chagas
Formal analysis: J. Moro, G. A. S. Picanço
Methodology: S. S. Chen, C. M. Denardini, L. C. A. Resende, R. A. J. Chagas
Writing – original draft: S. S. Chen
Writing – review & editing: S. S. Chen, C. M. Denardini, L. C. A. Resende, R. A. J. Chagas, J. Moro, G. A. S. Picanço

Abstract The Embrace Magnetometer Network (Embrace MagNet) uses a series of magnetometers over South America to monitor the Earth's space environment and to study space weather. One of the common techniques used to study the effects of the magnetic disturbances in the globe is through the quiet day curve (QDC) of the geomagnetic field components. These types of QDC are calculated based on geomagnetic field data collected by magnetometers in the five quietest days for each month at each station. Thus, we developed and implemented an empirical model based on the QDC *H* component obtained by the Embrace MagNet. This model ought to be used as a prediction device when data are not available. The proposed algorithm is a function of the solar activity, the day of the year, and the universal time, which was adjusted based on 12 stations across to the South America sector between 2010 and 2018. Our results show that the values computed by this model are in good agreement with the observational data for the QDC. Finally, it is essential to mention that the QDC model presented in this study is the only available predicting tool of the Embrace MagNet stations to date, providing data with a high confidence level in the Brazilian sector.

1. Introduction

It is well known that electrical current systems cause the daily variation of the Earth's magnetic field at the ionosphere due to the dynamo effect and the high conductivities (Campbell, 1989; Chapman, 1956; Chapman & Bartels, 1940; Maeda, 1966; Maeda & Kato, 1966; Matsushita, 1968; Yamazaki & Maute, 2017). This effect consists of the neutral atmosphere motion caused by the atmospheric tides which drag electron and ions along and across the magnetic field lines. Under geomagnetically quiet conditions (i.e., without magnetic disturbances caused by a solar flare, e.g., coronal mass ejection, and solar wind changes), the electrical currents are driven by the neutral particle movement caused by the neutral and tidal winds due to the high collision rates at the ionospheric *E* region heights. Thus, the nature of these currents can be separated into two main components: the solar quiet (Sq) and the lunar gravitational force (L).

The daily geomagnetic field variation is generally associated with the solar source (e.g., gravitational force and solar radiation), in which the dominating spectral components have periods of 24, 12, 8, and 6 hr (Campbell, 1989). These spectral components are related to the atmospheric oscillations of the neutral atmosphere parameters, such as pressure, wind, and temperature (Chapman & Lindzen, 1970). That variation describes a typical magnetic field signature on magnetograms named as quiet day curve (QDC) by Janzhura and Troshichev (2008). In this work, we also refer to the quiet daily geomagnetic field variations as QDC, which represents the daily mean variation of the geomagnetic field. There are few ways to characterize a typical daily variation, which we may also refer to as Sq variation.

The international quiet days and the international disturbed days are classifications of the 10 quietest days and 5 most disturbed days per month, respectively. These classifications are based on three criteria deduced from the *Kp* index described by Johnston (1943) and adopted by the International Association of Geomagnetism and Aeronomy to indicate the level of magnetic disturbances in a selected day compared to the other days of the same month. In general, the international quiet days exhibit rather smooth and regular daily changes that represent Sq variations (Yamazaki & Maute, 2017). Therefore, the typical Sq variation is based on the quietest days' average of the month. In most of the cases, the Sq variation is an average of the five quietest days of the month (Chapman & Bartels, 1940; Rastogi & Iyer, 1976).

Table 1
Stations Used in This Study

Station name	Station code	Geographic Lat. (°N)	Geographic Lon. (°E)	Geomagnetic quasi-dipole[a] Lat. (°N)	Geomagnetic quasi-dipole[a] Lon. (°E)
Manaus	MAN	−2.89	−59.97	4.23	13.40
Alta Floresta	ALF	−9.87	−56.10	−3.74	15.17
São Luís	SLZ	−2.59	−44.21	−3.82	27.73
Araguatins	ARA	−5.60	−48.10	−4.26	23.34
Eusébio	EUS	−3.88	−38.42	−8.02	32.55
Cuiabá	CBA	−15.55	−56.07	−8.68	13.87
Jataí	JAT	−17.93	−51.72	−12.69	16.92
Tucumán	TCM	−26.82	−65.19	−15.67	5.10
São José dos Campos	SJC	−23.21	−45.96	−19.65	20.50
Cachoeira Paulista	CXP	−22.70	−45.01	−19.71	21.39
Vassouras	VSS	−22.40	−43.65	−20.13	22.59
São Martinho da Serra	SMS	−29.44	−53.82	−21.32	13.36

[a]The geomagnetic quasi-dipole coordinates were obtained using the IGRF-13 for 1 January 2015.

Almost 30 years ago, worldwide distributions of the geomagnetic field daily variation were modeled by Campbell et al. (1989). However, their model does not contain a solar cycle adjustment, which may not represent the daily variation accurately with different solar fluxes. The accuracy of this model can be enhanced by considering more variables, such as geographic/geomagnetic coordinates; solar radio flux; seasonal, local time; and degree of geomagnetic activity dependence. However, no new model of the worldwide daily variations of the geomagnetic field has been developed hitherto.

Yamazaki et al. (2011) developed an empirical model of the daily geomagnetic field variation along the 210° magnetic meridian. This model was based on the least squares fitting method based on geomagnetic field data from 21 magnetic stations. A spherical harmonic analysis was performed to examine the solar and lunar variations. The results showed that the Sq current system is largely controlled by solar activity and seasonal variations exhibiting north-south asymmetry. The Northern Hemisphere vortex shows a prominent annual variation, whereas the southern vortex shows an apparent semiannual variation as well as an annual variation.

Janzhura and Troshichev (2008) presented an automatic method to obtain the daily variation in polar caps. With this method, it was possible to calculate a more realistic daily variation considering the effects of the northward interplanetary magnetic field in the quiet daily variation in these regions. More recently, Stauning (2011) showed a novel procedure to derive the QDC for polar caps based on the concept proposed by Janzhura and Troshichev (2008). They used a superposition analysis to estimate the QDC for any given day, using weighting functions to select intervals with the quietest conditions. They achieved a reliable and reproducible algorithm to compute the QDCs, which was considered by the authors a step forward in the processing of geomagnetic data given the difficulty related to high-latitude regions.

Regarding the daily variation models for the Southern Hemisphere, Sutcliffe (1999) developed a geomagnetic daily variation model of the horizontal component of Earth's magnetic field (H) by using artificial neural networks for the Southern African sector. Similarly, Unnikrishnan (2014) developed a model for the Indian regions, close to the dip equator. However, in these studies, the authors focused on predicting the H component behavior locally, which is yet not corresponding to the South American sector.

In South America, where the lowest intensity of the South America Magnetic Anomaly lies, there is a lack of models about the geomagnetic field daily variation during quiet periods. Thus, in this present work, we present a new empirical model of the QDC using the magnetometers covering mainly the Brazilian region. The new model encompasses the effects observed from our analysis of the solar cycle, day of the year, and time (in universal time, UT) based on the H component obtained from 12 stations in the South American sector from January 2010 to December 2018 to simulate the QDC variability. One of its advantages is that it can be easily expanded to cover the whole of Latin America in so far as we extend the Embrace Magnetometer Network (Embrace MagNet) proportionally and make it denser.

2. Methodology

We used the data set from the Embrace/INPE magnetometer network from 12 stations placed along with the South American sector, within a period ranging from 2010 to 2018. The Embrace MagNet uses fluxgate magnetometers that measure the variation of the Earth's magnetic field on the ground, with a 1-min time resolution calculated from 1-s data (Denardini et al., 2018a). We used the least squares fitting method to describe the QDC of the geomagnetic field horizontal component (H) as a function of the solar cycle, day of the year, and time.

Table 1 shows the description of the magnetic stations used in this work. These geomagnetic stations are part of the magnetometer network that belongs to the Brazilian Studies and Monitoring of Space Weather Program (Embrace). This network was established for scientific and space weather purposes in 2011 (Denardini et al., 2016). In this table, we present the station name, the code of each magnetic station, and its geographic and geomagnetic coordinates.

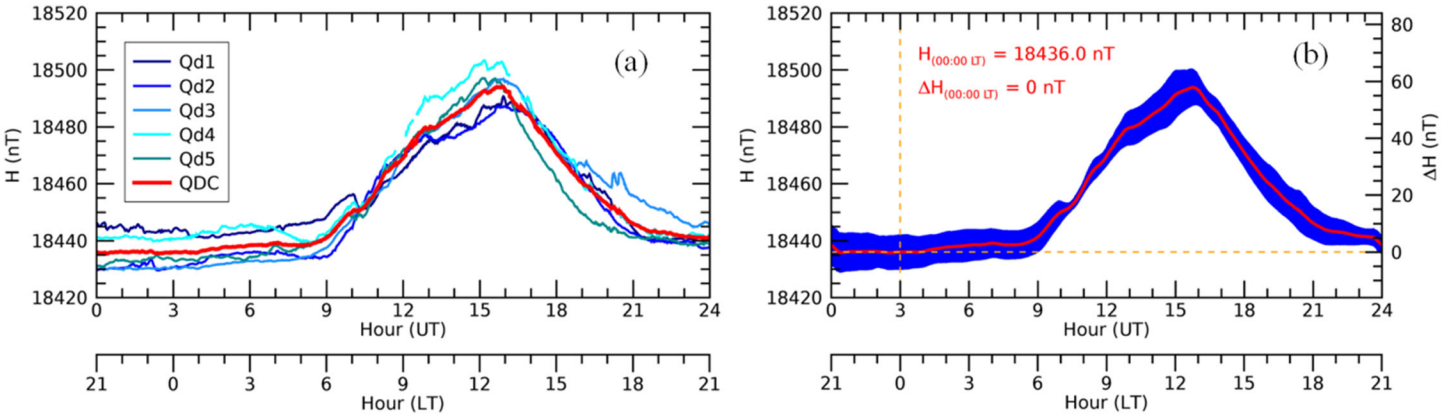

Figure 1. (a) The blue lines correspond to the daily variation of the geomagnetically quietest days in January 2014 for Cachoeira Paulista, and the red line indicates the mean daily variation or QDC. (b) The red line corresponds to the mean daily variation or QDC after smooth, and the blue area indicates the standard deviation (1σ).

The QDC calculation is constructed based on the Chapman and Bartels (1940) method, which characterizes the diurnal variation caused by solar atmospheric tides. In this method, the QDC is computed from the five quietest days in each month. These days are obtained on the GeoForschungsZentrum (GFZ) Helmholtz Centre Potsdam.

The QDC of the H component is given by Denardini et al. (2018b), after it evolved from the procedure for calibrating the network equipments as described by Denardini et al. (2015):

$$H_{QDC}(t) = \frac{1}{N}\sum_{i=1}^{5} H_{Qd_i}(t), \tag{1}$$

where H_{QDC} is the mean daily variation (QDC), H_{Qd_i} is the daily variation of the ith quietest day of the month, t is the time (UT) given with 1-min time resolution (from 00:00 up to 23:59 UT), and N is the number of days used in the calculation. In general, the number of days used to calculate the QDC is $N = 5$, but it can be fewer, depending on the data availability. Thus, we assumed a midnight zero-current level to obtain the amplitude of the QDC, which is also assumed to be the main field contribution around the local midnight hour:

$$\Delta H_{QDC}(t) = H_{QDC}(t) - H_{QDC}(00{:}00\ \mathrm{LT}), \tag{2}$$

where ΔH_{QDC} is the amplitude of the daily variation (QDC); H_{QDC} (00:00 LT) is the daily variation during local midnight, which is approximately the main field value or baseline; and t is the time like in the previous equation. We assumed the local midnight measurement to be the baseline since the nighttime ionization and ionospheric conductivity are lowest in the daily variation.

In this study, we used the data set comprising the period between September 2010 and December 2018, which covers the maximum and minimum phases of the solar cycle 24. We calculated the QDC for each station in Table 1. Figure 1 shows an example of the QDC computed for the Cachoeira Paulista station in January 2014. Figure 1a shows the daily variation of the quiet days (blue lines, Qd1, Qd2, Qd3, Qd4, and Qd5) and the QDC (in red line). Figure 1b shows the final result of the QDC, where the red line is QDC after smoothing and the blue area is its standard deviation (1σ). Notice that the daily variation during the local midnight has two significant values, which are indicated by the vertical and horizontal yellow dashed lines. The first value is what we assume to be the main field value or baseline, which is equal to H(00:00 LT) = 18,436 nT, and the second value is assumed to have no variation, which is equivalent to ΔH(00:00 LT) = 0 nT.

3. QDC Model

A method similar to that given in Yamazaki et al. (2011) is used to build our empirical model, in which the geomagnetic field daily variation is calculated through the least squares fitting of the observational data.

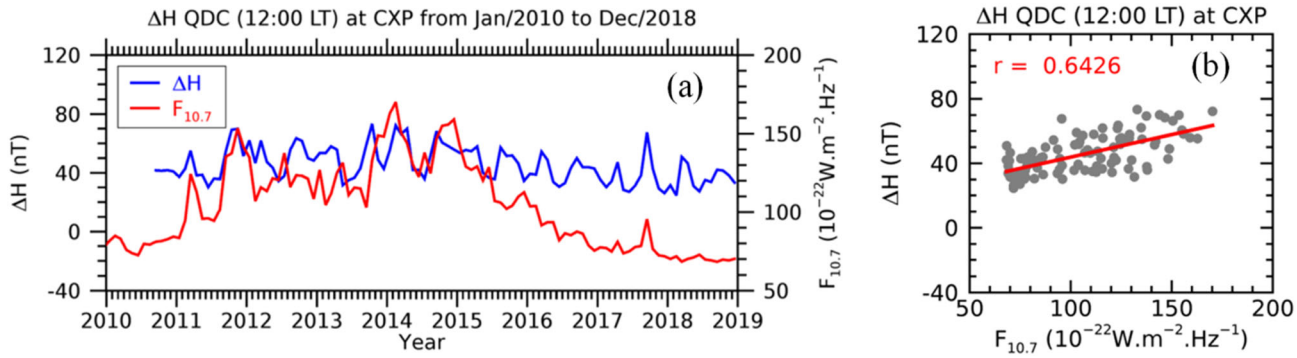

Figure 2. (a) Temporal series of ΔH_{QDC} at local midday (blue line) and the monthly value of $F_{10.7}$ (red line) from 2010 to 2018. (b) Linear correlation between ΔH_{QDC} and $F_{10.7}$.

Yamazaki et al. (2011) computed the Sq variations by using the quiet days ($Kp \leq 2+$) from the years 1996 until 2007. As these authors covered the 210° magnetic meridian, their model does not successfully describe the dynamics over South America, where the South America Magnetic Anomaly lies. In the following section, we describe the fitted parameters used to develop our QDC model, which were based on the solar cycle, seasonal, and daily variabilities.

3.1. Dependence on Solar Cycle Variation (*C*)

One of the parameters used to build our QDC model is the solar cycle variation, here referred to as *C*. The wavelength of the solar radio emission at 10.7 cm ($F_{10.7}$), which is given in solar flux units (1 sfu = 10^{-22} W·m^{-2}·Hz^{-1}), is commonly used to estimate the variability of the solar cycle since this parameter is directly related to the solar conditions (Bilitza, 2000; Liu et al., 2006).

Rastogi et al. (1994) showed a linear relationship between Sq amplitudes and $F_{10.7}$ in India, covering the period from 1975 to 1986. This observation was confirmed in Shinbori et al. (2017), in which they observed the same linear relationship between the Sq amplitude and the $F_{10.7}$ for the Memambetsu (43.91°N, 144.19°E) and Guam (13.59°N, 144.87°E) stations from 1957 to 2016.

To estimate the solar cycle variation and the Sq amplitude, we performed a linear fitting of the ΔH_{QDC} during local noon versus the solar radio flux over the 12 sites analyzed in this study. The monthly average of the solar radio flux is available online at the Natural Resources Canada database. An example is shown in Figure 2 for the Cachoeira Paulista station from the years 2010 to 2018. Figure 2a shows the time series of ΔH_{QDC} in 12:00 LT (blue line) and the monthly value of $F_{10.7}$ (red line). Figure 2b shows the correlation between these parameters. It is observed that the Pearson's correlation coefficient (*r*) was 0.64, which indicates a connection between the Sq amplitude and the solar radio flux. In fact, a low level of $F_{10.7}$ causes a decrease in the ΔH_{QDC} component, whereas the ΔH_{QDC} increases when $F_{10.7}$ is high over a low latitude (Rastogi et al., 1994).

Table 2
Solar Cycle Coefficients Obtained and Their Correlation

i	Code	C_0 (nT)	C_1 (nT/sfu)	*r*
A	MAN	−7.17	0.80	0.53
B	ALF	21.21	0.41	0.59
C	SLZ	23.85	0.27	0.68
D	ARA	−6.27	0.74	0.46
E	EUS	33.77	0.19	0.52
F	CBA	27.04	0.32	0.64
G	JAT	16.51	0.36	0.71
H	TCM	−20.81	0.71	0.52
I	SJC	14.07	0.23	0.60
J	CXP	15.83	0.28	0.64
K	VSS	14.25	0.27	0.42
L	SMS	6.96	0.26	0.71

The observed relationship between the Sq amplitude and the solar radiation is then approximated by the following:

$$C(F_{10.7}) = C_0 + C_1 F_{10.7}, \quad (3)$$

where C_0 and C_1 are coefficients of the solar cycle parameter, and $F_{10.7}$ is the solar radio flux given in solar flux units.

We performed this analysis to the other 11 geomagnetic stations, and the results are presented in Table 2. This table shows the station identifier *i*, followed by its code, the fitting coefficients C_0 and C_1 as described in Equation 3, and the Pearson's correlation coefficient *r*. In general, for all stations analyzed here, the correlation between the Sq amplitude and the $F_{10.7}$ showed a clear dependence on the solar cycle, agreeing

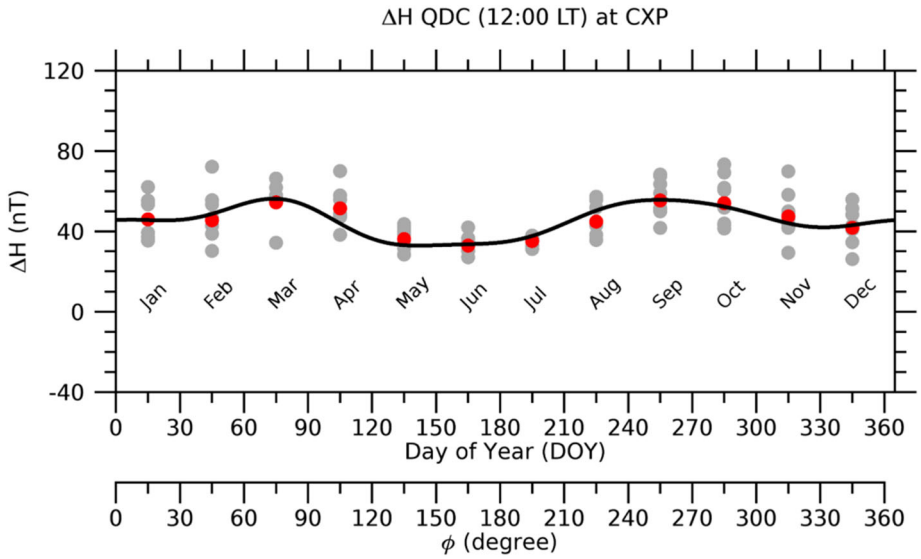

Figure 3. Temporal series of the ΔH_{QDC} at local midday at Cachoeira Paulista.

with the results presented by Shinbori et al. (2014). The C_0 coefficients observed for MAN, ARA, and TCM are negative, being more expressive in the TCM station. Those negative values are related to a short time series of magnetic field data during the minimum solar cycle 24 (from about 1 to 2 years of data). In those cases, the observational data span across the abscissa is short, leading to estimation accuracy degradation in the linear fitting process due to possible outliers.

3.2. Dependence on Seasonal Variation (*S*)

The seasonal variation features and their importance in the Sq current systems are already well known (Matsushita & Maeda, 1965; Rastogi et al., 1994; Takeda, 2013). The seasonality parameter (referred to as *S*) is associated with the variation along the day of the year. Therefore, we based on the harmonic analysis of the atmospheric oscillations described by Chapman and Lindzen (1970).

An example of how we included the *S* parameter in the QDC model is shown in Figure 3. The ΔH_{QDC} values computed at 12:00 LT at the Cachoeira Paulista station were split by the year and merged into a single time series (gray dots), centered in the middle day of the corresponding month. The red dots are the ΔH_{QDC} monthly averaged. The black line corresponds to a Fourier series fitting of the red dots. The vertical axis indicates the *H* component magnitude of the variation, and the horizontal axis indicates the day of the year (*DOY*) or a 360° variation in ϕ for amplitudes of a cyclic variation. Notice that the ΔH_{QDC} shows a semiannual seasonal variation with two maximums close to March and September equinoxes, agreeing with the expected behavior for equatorial and low-latitude regions (Matsushita & Maeda, 1965; Rastogi & Iyer, 1976; Campbell, 1982; Okeke & Hamano, 2000).

We included the seasonal variation *S* in the QDC model using the following:

$$S(DOY) = S_0 + \sum_{j=1}^{N} S_j \cos\left(2\,\pi j DOY + \phi_j\right), \tag{4}$$

where S_0 up to S_N are coefficients obtained from the Fourier series fitting, *j* is the number of the *j*th harmonic, ϕ_j is the phase angle of the *j*th harmonic, and *DOY* is the day of the year given in decimal. For the current

Table 3
Amplitude and Phase Angles Obtained From the Fourier Series Expansion for the Seasonality Parameter at the Cachoeira Paulista Station

Parameter	$j = 0$	$j = 1$	$j = 2$	$j = 3$	$j = 4$	$j = 5$	$j = 6$
S_j (nT)	64.20	4.97	8.84	0.95	1.97	1.43	0.47
ϕ_j (rad)	0	0.6197	−2.3852	1.4840	0.8880	−0.4710	0

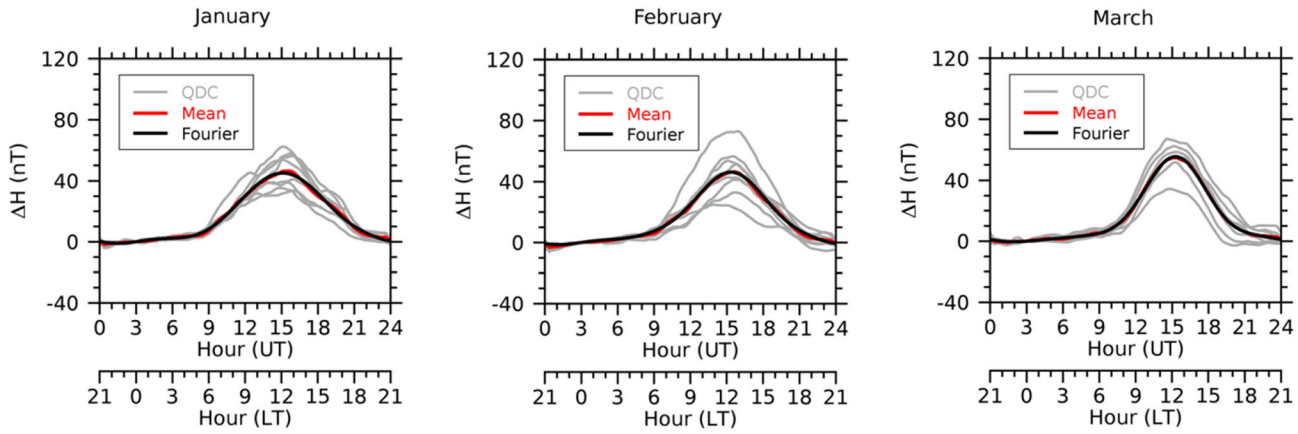

Figure 4. The daily variation of the ΔH_{QDC} obtained from January to March at Cachoeira Paulista.

model, six harmonics, i.e., $N = 6$, provided sufficient smoothing with an adequate approximation to the expected theoretical behavior. The coefficients obtained for the Cachoeira Paulista station are summarized in Table 3.

3.3. Dependence on Daily Variation (D_m)

The daily variation (D_m) exhibits oscillations with periods of 24, 12, 8, and 6 hr in the ionosphere at low height (Campbell, 2003). These period oscillations are related to the atmospheric tides described by Chapman and Lindzen (1970). The diurnal and semidiurnal tides (24- and 12-hr periods) are the most important components in the equatorial and low-latitude E region dynamics (around 100- to 110-km altitude) (Andrioli et al., 2009; Resende et al., 2017, 2018). The terdiurnal tides are related to nonlinear interaction between diurnal and semidiurnal tides, and it can occur in low latitudes (Tokumoto et al., 2007). The quarterdiurnal tides are the less intense between those tides, influencing the E region behavior during the winter solstice (Guharay et al., 2018).

For the QDC model, we computed the daily variation of the Sq current system by fitting the data using the Fourier series expansion as in the following:

$$D_m(UT) = D_{m,0} + \sum_{n=1}^{N} D_{m,n}\cos\left(2\pi f_n UT + \phi_{m,n}\right), \quad (5)$$

where m corresponds to the selected month, $D_{m,0}$ up to $D_{m,n}$ are the fitted coefficients, f_n is the frequency of the nth harmonic, $\phi_{m,n}$ is the phase angle of the nth harmonic, and UT is the time (in universal time)

Table 4
Daily Variation Coefficients Obtained for the Cachoeira Paulista Station

	$D_{m,n}$ (nT)					$\phi_{m,n}$ (rad)			
m	$n = 0$	$n = 1$	$n = 2$	$n = 3$	$n = 4$	$n = 1$	$n = 2$	$n = 3$	$n = 4$
1	22.62	21.75	6.69	0.99	0.28	2.3421	−1.6970	1.3943	1.2812
2	20.36	21.01	7.88	1.98	0.64	2.3332	−1.8382	0.6425	2.5634
3	22.14	23.04	11.08	4.56	1.06	2.3054	−1.7379	0.6308	2.6628
4	18.68	19.94	10.38	5.22	1.51	2.5461	−1.3680	0.9665	2.8878
5	14.75	14.37	7.06	4.30	1.13	2.5539	−1.0234	1.3644	3.0756
6	13.34	13.57	6.29	3.41	0.98	2.5678	−1.1167	1.3461	2.9225
7	15.95	14.62	5.87	3.54	0.73	2.4299	−1.2052	1.3264	2.8274
8	17.16	17.72	8.84	4.64	1.43	2.4462	−1.4041	0.9864	2.6975
9	20.78	22.15	11.30	5.94	2.13	2.4771	−1.4197	0.9169	2.6410
10	22.74	23.85	10.04	3.96	1.09	2.3354	−1.5725	1.0535	2.8959
11	22.12	22.67	8.17	1.69	0.48	2.3882	−1.5752	1.0637	1.4834
12	20.91	20.42	6.67	1.01	0.79	2.3634	−1.7361	0.8328	0.9534

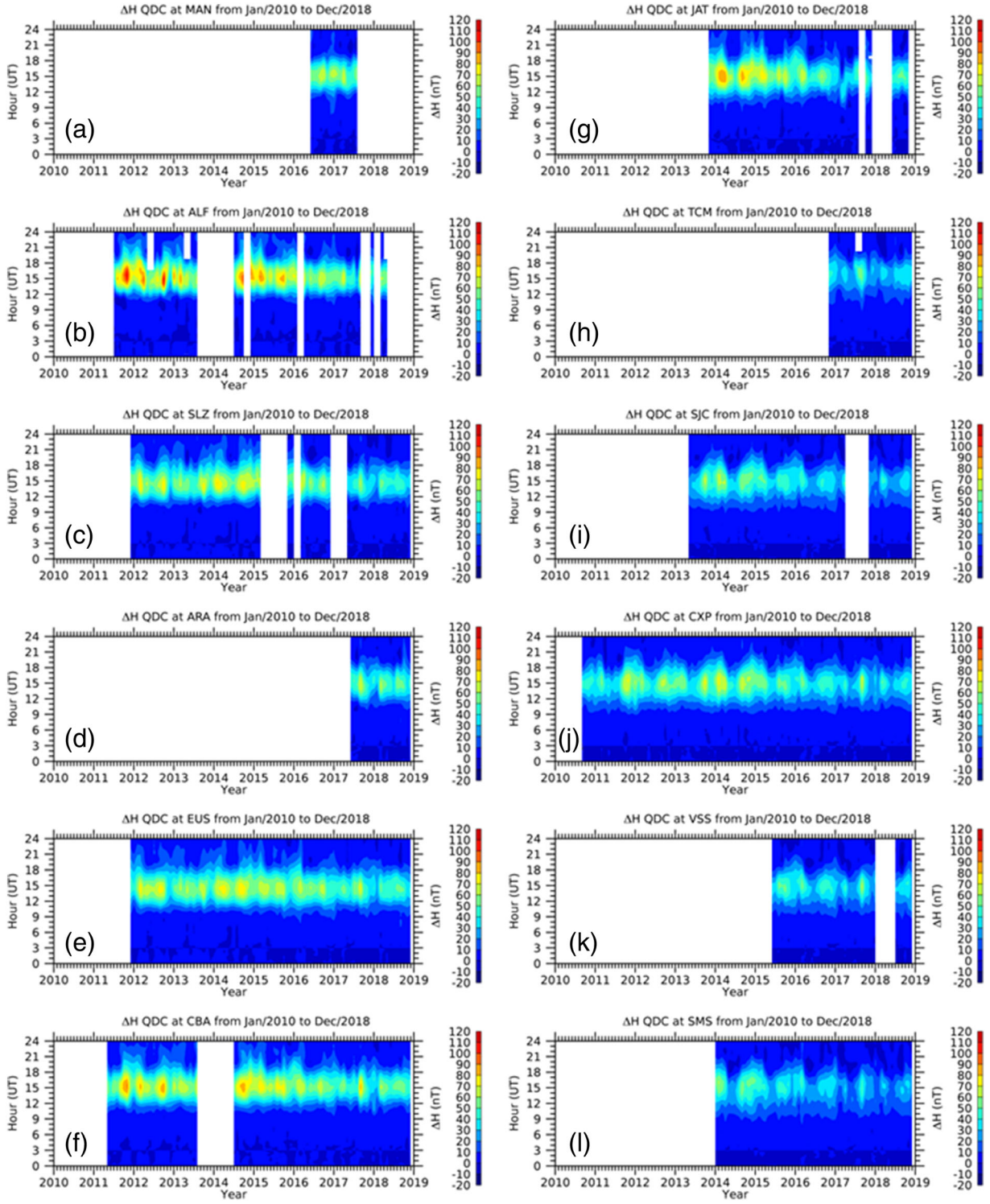

Figure 5. Time series of the monthly QDC (in universal time) obtained from the geomagnetic field data measured by the Embrace MagNet stations for the years 2010–2018, arranged in a map format.

given in decimal hours. In this case, we used four harmonics, i.e., $N = 4$. Notice that these parameters were calculated individually for each month. In the following, we present an example of how this was performed for the Cachoeira Paulista station.

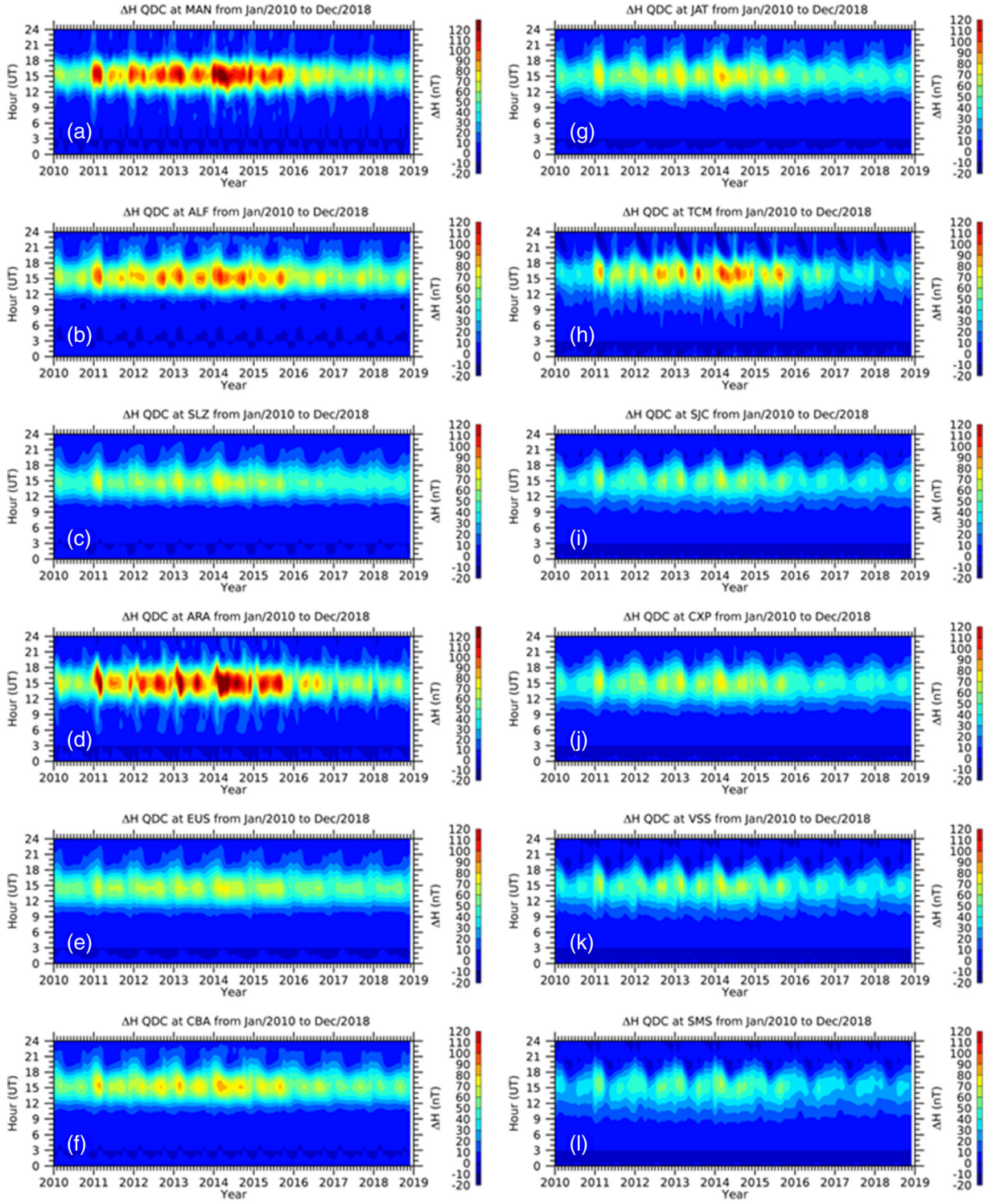

Figure 6. Time series of the monthly QDC (in universal time), similar to those of Figure 5, but obtained by the empirical model over the same location of the Embrace MagNet stations for the years 2010–2018, arranged in a map format.

Figure 4 shows examples of the daily variation for 3 months (January, February, and March). The gray lines correspond to the QDC data derived from Equation 2. The red lines are monthly averages of the QDC, which was computed from the magnetic field data. The black line indicates the fitted curve, which was applied for all months of the year. Table 4 summarizes the coefficients obtained from this analysis.

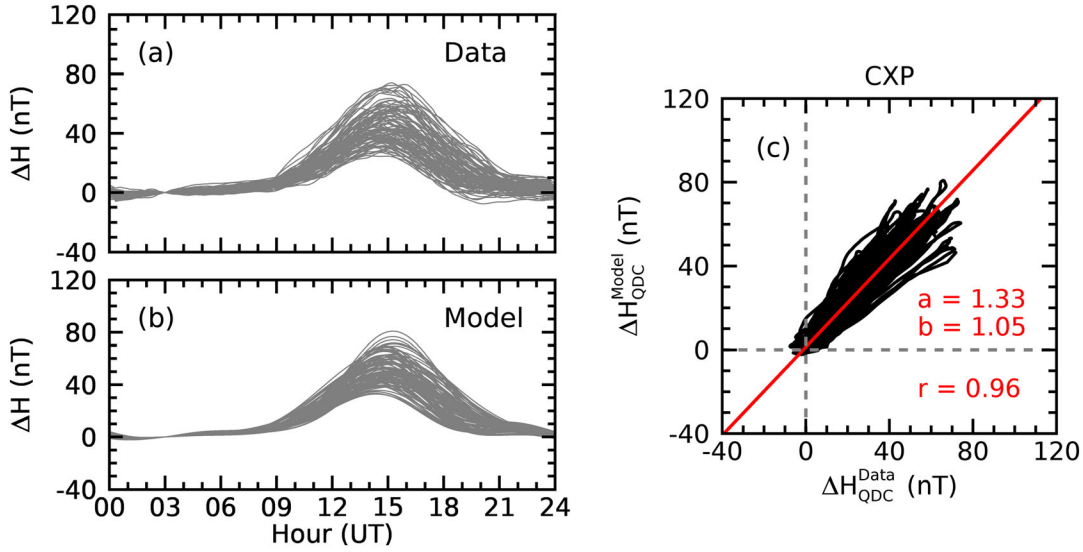

Figure 7. (a) Monthly QDC distribution obtained from the geomagnetic field data from the years 2010 up to 2018 over Cachoeira Paulista. (b) Monthly QDC distribution similar to that of Figure 7a but obtained by the empirical model over the same location. (c) Linear correlation between the QDC modeled and the QDC of the observational data.

3.4. Sq Variation

Considering the three above mentioned modeled parameters (C, S, and D_m), the Sq variation is given by

$$\Delta H_{QDC}(F_{10.7}, DOY, UT) = C(F_{10.7}).S(DOY).D_m(UT), \quad (6)$$

where C is the solar cycle, S is the seasonality, and D_m is the daily variation. Notice that the C parameter is given in nT, and S and D_m are adimensional parameters normalized by relative values of the Sq amplitude. We normalize the seasonal and daily parameters to obtain their relative geomagnetic field variations.

4. Results and Discussions

4.1. Comparison Between Observational Data and Model Output

Figure 5 shows the QDC maps, similar to those presented in Figure 3 by Denardini et al. (2018b), over the 12 magnetic stations indicated by a letter from A to L. The vertical and horizontal axes are the hours in universal time (UT) and the years, respectively. The color range in the right of each panel corresponds to the ΔH magnitude. The white space in the maps indicates the absence of data.

The eastward direction of the Sq current system is seen as the increase in the magnitude of the H component, observed in Figure 5. The typical behavior of the QDCs in all stations is a peak in the ΔH around the local noon, which is cyclical for each year. We observe that after the semiannual peaks in the equinox months, the QDC presents lower values in the solstice months. Additionally, we see that the most significant variations of the daytime variation occur between 09:00 UT and 21:00 UT for equinoxes and summer. During winter (June, July, and August), these oscillations are more significant between 12:00 UT and 18:00 UT. This daytime variation is related to seasonality and occurs due to the corresponding solar incidence in the atmosphere over the stations.

Figure 6 shows the maps of Sq amplitude values produced by the model as they are obtained from Equation 6. The identification, color scales, axis orientation, and map distribution are the same as those presented in Figure 5. Thus, comparing these outputs vis-à-vis with the monthly QDC obtained from the data, we can see that the model successfully simulated the QDC, reaching a maximum value at around local noon. Also, the simulated QDC showed that the most significant variations are in the daytime, agreeing with the observational data behavior. The stations with the highest correlation between data and modeling outputs were Alta Floresta (B), São Luís (C), Eusébio (E), Cuiabá (F), Jataí (G), São José dos Campos (I), Cachoeira Paulista (J), Vassouras (K), and São Martinho da Serra (L).

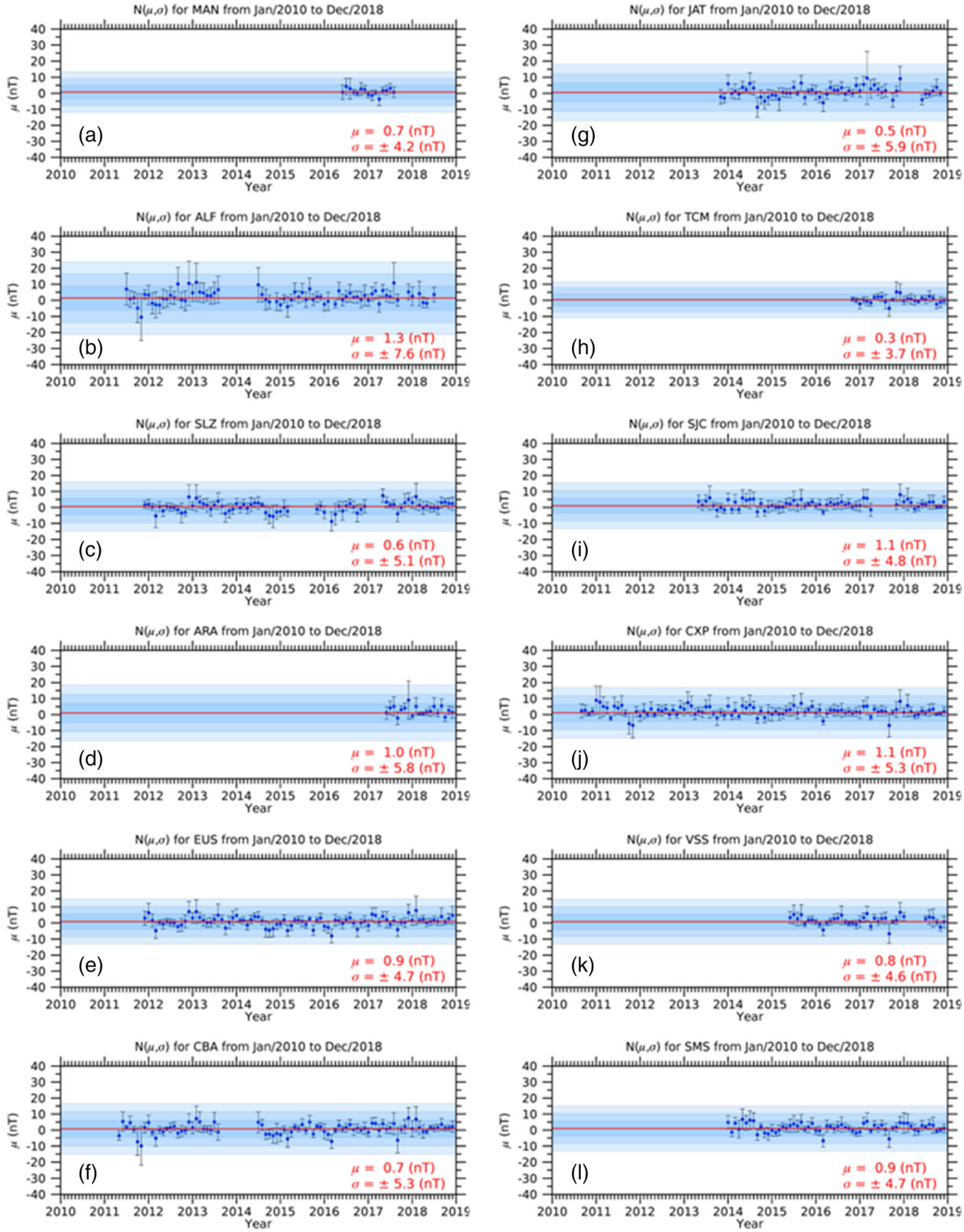

Figure 8. Error of the empirical model obtained over the same location of the Embrace MagNet stations for the years 2010–2018. The blue dots are the total error of each QDC (μ_k), and the vertical bars correspond to its standard deviation ($\pm\sigma_k$). The mean error is indicated by μ in red, and the blue shaded areas corresponds to the intervals $\pm\sigma$, $\pm2\sigma$, and $\pm3\sigma$.

Table 5
Computed Total Error of Each Magnetic Station Modeled

i	Station code	Computed errors μ (nT)	σ (nT)
A	MAN	0.7	4.2
B	ALF	1.3	7.6
C	SLZ	0.6	5.1
D	ARA	1.0	5.8
E	EUS	0.9	4.7
F	CBA	0.7	5.3
G	JAT	0.5	5.9
H	TCM	0.3	3.7
I	SJC	1.1	4.8
J	CXP	1.1	5.3
K	VSS	0.8	4.6
L	SMS	0.9	4.7
Average		0.8	5.1

There are few discrepancies observed between the empirical model and the observational data, however. The differences are noticed at the magnetic stations of Manaus (A), Araguatins (D), and Tucumán (H). For these magnetic stations, the model overestimated the observational data. Nevertheless, the more substantial differences occur during the solar maximum when we do not have enough data to obtain the QDC properly. Therefore, the model works better during the minimum phase of the solar cycle in these stations, which is clearly observed later in 2016.

Overall, the model is capable of reproducing a significant correlation between the QDC and the solar cycle variation. In both data and simulations, it is possible to observe the higher (lower) values lying around the solar maximum (minimum). Takeda (2013) studied the long-term variations in the Sq amplitude and the effects of solar activity considering several observatories for about 50 years. His results showed that solar activity strongly influences the Sq current in all observatories, causing an increase in the *E* region ionospheric conductivity. Therefore, during the solar maximum, the field-aligned currents driven by the Sq dynamo increase, leading the solar quiet geomagnetic field variations to present higher values.

In order to provide a more detailed view of the amplitude of the QDCs obtained from observational data collected in Cachoeira Paulista with the empirical model outputs, we present Figure 7. Notice that Figures 7a and 7b show QDCs obtained from the observational data and the empirical model, respectively. This station presents the best agreement between the maximum and minimum amplitudes in comparison with those of other stations. We credit this fact to the long-term time series of geomagnetic field data available. Also, from 2016, we noted a decrease in the magnitude of the QDCs in both observational data and model. This behavior occurs because these years are in the solar minimum, as shown before through $F_{10.7}$ (see Figure 2). This conduct is observed in all stations of this analysis, showing that the solar cycle effect was simulated correctly. Figure 7c shows the linear correlation between the QDC obtained from the observational data and the empirical model in Cachoeira Paulista, in which Pearson's correlation coefficient ($r = 0.96$) shown a high confidence interval. The linear regression obtained from this correlation shows that the QDCs modeled overestimate about 5% ($b = 1.05$) the observational data, and with a bias of $a = 1.33$ nT.

Therefore, in general, we noticed that the results of simulations are practically similar to the observational data, with low variations occurring between 09 UT and 21 UT. The main difference is related to the time delay between the shapes of the curves. We quantify the error of the model in the next section.

4.2. Analysis of the Errors in the Parameters

In order to quantify the error of the model and to support the results presented in the previous sections, we used the following methodology to determine the average error when comparing the model output with the data set. Assuming that the error can be described by a Gaussian distribution, the mean error (μ) can be computed using the inverse-variance weighting as (Papoulis & Pillai, 2016)

$$\mu = \frac{\sum_{k=1}^{N} \mu_k / \sigma_k^2}{\sum_{k=1}^{N} 1/\sigma_k^2}, \tag{7}$$

and it can be proven that the standard deviation σ can be computed by

$$\sigma^2 = \frac{1}{N} \sum_{k=1}^{N} \left(\mu_k^2 + \sigma_k^2\right) - \mu^2, \tag{8}$$

where μ_k is the mean error of each kth observation point, which is obtained from the average difference between the model result and the QDC measurement. Similarly, σ_k is the standard deviation of each observation point. Notice that the latter is increased by, among other effects, the magnetometer measurement errors, meaning that this is a conservative approach.

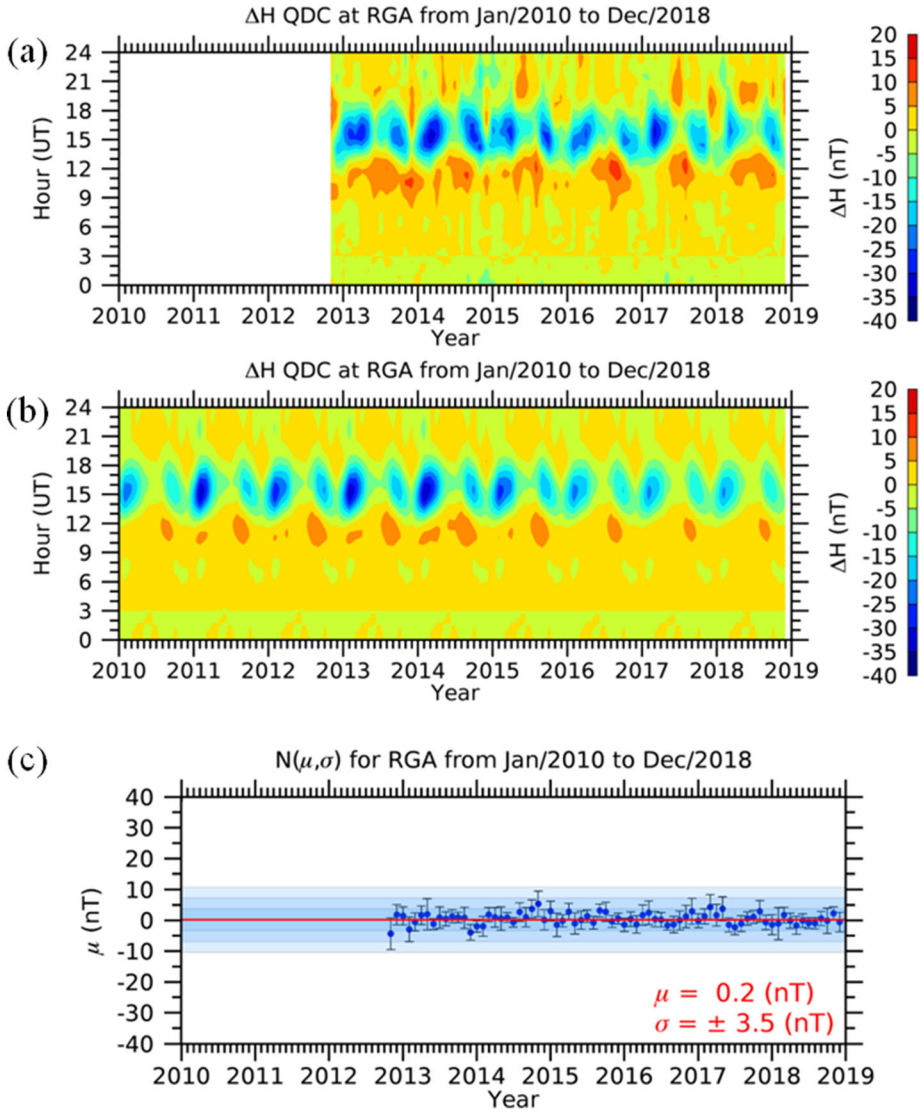

Figure 9. (a) Monthly QDC distribution obtained from the geomagnetic field data from the years 2010 up to 2018 over Rio Grande. (b) Monthly QDC distribution similar to that in Figure 9a but obtained by the empirical model over the same location. (c) The error of the empirical model for the Rio Grande station. The mean (μ) value is indicated in the red line, and the blue shaded area corresponds to the intervals $\pm\sigma$, $\pm 2\sigma$, and $\pm 3\sigma$.

Using this procedure, we computed the modeling error statistics for each station separately, as shown in Figure 8. The vertical axis is the modeling error in nT, and the horizontal axis is the time in years divided by months. The blue dot is the mean μ_k, whereas the error bars indicate the interval $\pm\sigma_k$. The red line represents the compound error μ (Equation 7), and the three blue shaded areas are related to the intervals $\pm\sigma$, $\pm 2\sigma$, and $\pm 3\sigma$ (Equation 8). The resulting averaged errors per station are listed in Table 5.

The data show that the mean modeling error is small. The highest value was 1.3 nT at ALF. This observation indicates that the model can be considered unbiased; i.e., the systematic error is negligible. Thus, it can be concluded that all major factors that have an impact on the Sq variation were successfully taken into account by the proposed model. The standard deviation is also relatively small but presented some variation across the analyzed stations. However, this is a random behavior that can be explained by measurement errors or local perturbations in the magnetometer network.

Furthermore, we tested our model for Rio Grande, Argentina (−53.79°N, −67.76°E, RGA), a station located on the other side of the vortex, where the Sq currents flow in the westward direction in the Southern Hemisphere. The results are shown in Figure 9. Figure 9a shows the observational data, and the

simulations data is seen in Figure 9b. Notice that the behavior of the ΔH magnitude on RGA measurements is quite different from that on the other magnetic stations. In other words, at 15:00 UT (12:00 LT), we observed a minimum in the H component amplitude, which is associated with the westward current. However, positive values are observed in the H component earlier in the morning, around 12:00 UT (09:00 LT), which also means that the Sq current system flows in the eastward direction, too. Therefore, RGA may be close to the Sq current system focus in the southern vortex. Regarding the results of Figure 9b, we notice that the model was capable of simulating the behavior of this station. The error placed in Figure 9c is even less significant than that in the other stations presented before. In some hours, it was possible to observe that the model overestimated the results. This fact is confirmed because, although small, the mean error is positive.

Finally, the results presented in this work show that the QDC model satisfactorily simulates the daily variation of the H component. It is possible to mention that this model provides a complete set of results for the QDC over low latitudes. Thus, the QDC model presented in this study is the only available predicting tool of the Embrace MagNet stations to date that provide data with a high confidence level in the Brazilian sector.

5. Conclusions

We developed and implemented an empirical model of the Sq variation above the Earth's surface over the South American sector to simulate the QDC. This model was built in terms of solar activity, day of the year, and universal time using magnetic data collected at 12 stations along to the South American sector from the years 2010 up to 2018. We conducted a careful analysis of the data and also compared the results with simulations obtained from this new model, leading to the following main conclusions:

1. Concerning the magnetometer data, which are used to calculate the QDC, the results show a typical behavior in all stations analyzed, with peaks around the local noon. We observe that the ΔH peak presents a decrease over the years later in 2015. Additionally, we see that the most significant variations of the daytime variation occur between 09:00 UT and 21:00 UT for equinoxes and summer. In winter, these oscillations are more significant between 12:00 UT and 18:00 UT. This daytime variation is related to seasonality and occurs due to the significant time of the solar incidence in the atmosphere.
2. In general, the observational behavior was satisfactorily simulated in the QDC model. We noticed that the results of simulations are practically similar to the observational data, with variations occurring between 09:00 UT and 21:00 UT.
3. Also, the model was capable of reproducing the significant correlation between the QDC and the solar cycle. In both data and simulations, it is possible to observe the higher (lower) values around the solar maximum (minimum), which agree with previous studies once the solar activity has a strong influence on the Sq current, affecting the ionospheric conductivity in the E region and, in turn, the field-aligned currents driven by the Sq dynamo.
4. The main difference between the QDC data and the QDC modeled is related to the time delay between the shapes of the curves. This feature is attributed to the parameters used in this model. Therefore, we quantify the error of the model to identify possible inaccuracy sources. The data show that the mean modeling error is small. The highest value was 1.3 nT at ALF, which lies close to the resolution of the magnetometer offset. This observation indicates that the model can be considered unbiased; i.e., the systematic error is negligible.
5. We tested our model for a region located on the other side of the vortex, RGA, where the Sq currents flow in the westward direction in the South Hemisphere. We observe a minimum of H component amplitude, which is associated with the westward current, but positive values are seen in the morning around 12:00 UT (09:00 LT), which also means that the Sq current system flows in the eastward direction, too. The QDC model was capable of simulating the behavior of this station in most of the hours. The discrepancies were observed mainly during the morning when the simulations overestimate the results.
6. Finally, we concluded that all major factors that have an impact on the Sq variation were successfully taken into account by the proposed model. The standard deviation is also relatively small across the analyzed stations (5.1 nT on average). However, this is a random behavior that can be explained by measurement errors or local perturbations in the magnetometer network. Therefore, the QDC model presented in

this study is the only available model of the Embrace MagNet stations that can allow predicting, with a high confidence level in the Brazilian sector.

Acknowledgments
S. S. Chen is grateful to CNPq/MCTIC (grant 134151/2017-8) and CAPES/MEC (grant 88887.362982/2019-00). C. M. Denardini thanks CNPq/MCTIC (grant 303643/2017-0). L. C. A. Resende is grateful to China-Brazil Joint Laboratory for Space Weather (CBJLSW), National Space Science Center (NSSC), Chinese Academy of Sciences (CAS), for supporting her postdoctoral fellowship. J. Moro is grateful to China-Brazil Joint Laboratory for Space Weather (CBJLSW), National Space Science Center (NSSC), Chinese Academy of Sciences (CAS), for supporting his postdoctoral fellowship and to CNPq/MCTIC (grant 429517/2018-01). G. A. S. Picanço thanks CAPES/MEC (grant 88887.467444/2019-00). The authors acknowledge Embrace/INPE for providing the magnetic data (http://www.inpe.br/spaceweather/), GFZ Potsdam for the classification of International Q-Days (ftp://ftp.gfz-potsdam.de/pub/home/obs/kp-ap/quietdst/), and Natural Resources Canada (NRC) for providing the solar radio flux data (https://www.spaceweather.gc.ca/solarflux/sx-en.php).

References

Andrioli, V. F., Clemesha, B. R., Batista, P. P., & Schuch, N. J. (2009). Atmospheric tides and mean winds in the meteor region over Santa Maria (29.7°S; 53.8°W). *Journal of Atmospheric and Solar-Terrestrial Physics*, *71*(17), 1864–1876. https://doi.org/10.1016/j.jastp.2009.07.005

Bilitza, D. (2000). The importance of EUV indices for the international reference ionosphere. *Physics and Chemistry of the Earth – Part C*, *25*(5–6), 515–521. https://doi.org/10.1016/S1464-1917(00)00068-4

Campbell, W. H. (1982). Annual and semiannual changes of the quiet daily variations (Sq) in the geomagnetic field at North American locations. *Journal of Geophysical Research*, *87*(A2), 785–796. https://doi.org/10.1029/JA087iA02p00785

Campbell, W. H. (1989). An introduction to quiet daily geomagnetic fields. *Pure and Applied Geophysics*, *131*(3), 315–331. https://doi.org/10.1007/BF00876831

Campbell, W. H. (2003). *Introduction to geomagnetic fields*. Cambridge: Cambridge University Press.

Campbell, W. H., Schiffmacher, E. R., & Kroehl, H. W. (1989). Global quiet day field variation model WDCA/SQ1. *Eos, Transactions of the American Geophysical Union*, *70*(5), 66–74. https://doi.org/10.1029/89eo00039

Chapman, S. (1956). The electrical conductivity of the ionosphere: A review. *Nuovo Cimento*, *4*(4), 1385–1412. https://doi.org/10.1007/BF02746310

Chapman, S., & Bartels, J. (1940). *Geomagnetism* (Vol. 1). London: Oxford University Press.

Chapman, S., & Lindzen, R. S. (1970). *Atmospheric tides: Thermal and gravitational*. Dordrecht: Springer. https://doi.org/10.1007/978-94-010-3399-2

Denardini, C. M., Chen, S. S., Resende, L. C. A., Moro, J., Bilibio, A. V., Fagundes, P. R., et al. (2018a). The embrace magnetometer network for South America: Network description and its qualification. *Radio Science*, *53*, 288–302. https://doi.org/10.1002/2017RS006477

Denardini, C. M., Chen, S. S., Resende, L. C. A., Moro, J., Bilibio, A. V., Fagundes, P. R., et al. (2018b). The embrace magnetometer network for South America: First scientific results. *Radio Science*, *53*, 379–393. https://doi.org/10.1002/2018RS006540

Denardini, C. M., Dasso, S., & Gonzalez-Esparza, J. A. (2016). Review on space weather in Latin America. 2. The research networks ready for space weather. *Advances in Space Research*, *58*(10), 1940–1959. https://doi.org/10.1016/j.asr.2016.03.013

Denardini, C. M., Silva, M. R. D., Gende, M. A., Chen, S. S., Fagundes, P. R., Schuch, N. J., et al. (2015). The initial steps for developing the South American K index from the embrace magnetometer network. *Brazilian Geophysics Journal*, *33*(1), 79–88. https://doi.org/10.22564/rbgf.v33i1.603

Guharay, A., Batista, P. P., Buriti, R. A., & Schuch, N. J. (2018). On the variability of the quarter-diurnal tide in the MLT over Brazilian low-latitude stations. *Earth, Planets and Space*, *70*(1), 1–14. https://doi.org/10.1186/s40623-018-0910-9

Janzhura, A. S., & Troshichev, O. A. (2008). Determination of the running quiet daily geomagnetic variation. *Journal of Atmospheric and Solar-Terrestrial Physics*, *70*(7), 962–972. https://doi.org/10.1016/j.jastp.2007.11.004

Johnston, H. F. (1943). Mean K-indices from twenty-one magnetic observatories and five quiet and five disturbed days for 1942. *Terrestrial Magnetism and Atmospheric Electricity*, *48*(4), 219–227. https://doi.org/10.1029/TE048i004p00219

Liu, L., Wan, W., Ning, B., Pirog, O. M., & Kurkin, V. I. (2006). Solar activity variations of the ionospheric peak electron density. *Journal of Geophysical Research*, *111*, A08304. https://doi.org/10.1029/2006JA011598

Maeda, H. (1966). Generalized dynamo mechanism in the upper atmosphere. *Journal of Geomagnetism and Geoelectricity*, *18*(2), 173–182. https://doi.org/10.5636/jgg.18.173

Maeda, K., & Kato, S. (1966). Electrodynamics of the ionosphere. *Space Science Reviews*, *5*(1), 57–79. https://doi.org/10.1007/BF00179215

Matsushita, S. (1968). *Sq* and *L* current systems in the ionosphere. *Geophysical Journal of the Royal Astronomical Society*, *15*(1-2), 109–125. https://doi.org/10.1111/j.1365-246X.1968.tb05751.x

Matsushita, S., & Maeda, H. (1965). On the geomagnetic solar quiet daily variation field during the IGY. *Journal of Geophysical Research*, *70*(11), 2535–2558. https://doi.org/10.1029/jz070i011p02535

Okeke, F. N., & Hamano, Y. (2000). Daily variations of geomagnetic *H*, *D* and *Z*-field at equatorial latitudes. *Earth, Planets and Space*, *52*(4), 237–243. https://doi.org/10.1186/BF03351632

Papoulis, A., & Pillai, S. U. (2016). *Probability, random variables, and stochastic processes*. New York, USA: McGraw Hill.

Rastogi, R. C., Alex, S., & Patil, A. (1994). Seasonal variations of geomagnetic *D*, *H* and *Z* fields at low latitudes. *Journal of Geomagnetism and Geoelectricity*, *46*(2), 115–126. https://doi.org/10.5636/jgg.46.115

Rastogi, R. C., & Iyer, K. N. (1976). Quiet day variation of geomagnetic *H*-field at low latitudes. *Journal of Geomagnetism and Geoelectricity*, *28*(6), 461–479. https://doi.org/10.5636/jgg.28.461

Resende, L. C. A., Batista, I. S., Denardini, C. M., Batista, P. P., Carrasco, A. J., Andrioli, V. F., & Moro, J. (2017). Simulations of blanketing sporadic E-layer over the Brazilian sector driven by tidal winds. *Journal of Atmospheric and Solar-Terrestrial Physics*, *154*, 104–114. https://doi.org/10.1016/j.jastp.2016.12.012

Resende, L. C. A., Batista, I. S., Denardini, C. M., Batista, P. P., Carrasco, A. J., Andrioli, V. F., & Moro, J. (2018). The influence of tidal winds in the formation of blanketing sporadic E-layer over equatorial Brazilian region. *Journal of Atmospheric and Solar-Terrestrial Physics*, *171*, 64–71. https://doi.org/10.1016/j.jastp.2017.06.009

Shinbori, A., Koyama, Y., Nosé, M., Hori, T., & Otsuka, Y. (2017). Characteristics of seasonal variation and solar activity dependence of the geomagnetic solar quiet daily variation. *Journal of Geophysical Research: Space Physics*, *122*, 10,796–10,810. https://doi.org/10.1002/2017JA024342

Shinbori, A., Koyama, Y., Nosé, M., Hori, T., Otsuka, Y., & Yatagai, A. (2014). Long-term variation in the upper atmosphere as seen in the geomagnetic solar quiet daily variation. *Earth, Planets and Space*, *66*(1), 1–20. https://doi.org/10.1186/s40623-014-0155-1

Stauning, P. (2011). Determination of the quiet daily geomagnetic variations for polar regions. *Journal of Atmospheric and Solar-Terrestrial Physics*, *73*(16), 2314–2330. https://doi.org/10.1016/j.jastp.2011.07.004

Sutcliffe, P. R. (1999). The development of a regional geomagnetic daily variation model using neural networks. *Annales Geophysicae*, *18*(1), 120–128. https://doi.org/10.1007/s00585-000-0120-0

Takeda, M. (2013). Difference in seasonal and long-term variations in geomagnetic Sq fields between geomagnetic Y and Z components. *Journal of Geophysical Research: Space Physics*, *118*, 2522–2526. https://doi.org/10.1002/jgra.50128

Tokumoto, A. S., Batista, P. P., & Clemescha, B. R. (2007). Terdiurnal tides in the MLT region over Cachoeira Paulista (22.7°S; 45°W). *Brazilian Journal of Geophysics*, *25*, 69–78. https://doi.org/10.1590/S0102-261X2007000600009

Unnikrishnan, K. (2014). Prediction of horizontal component of Earth's magnetic field over Indian sector using neural network model. *Journal of Atmospheric and Solar-Terrestrial Physics*, *121*, 206–220. https://doi.org/10.1016/j.jastp.2014.06.014

Yamazaki, Y., & Maute, A. (2017). Sq and EEJ—A review on the daily variation of the geomagnetic field caused by ionospheric dynamo currents. *Space Science Reviews*, *206*(1–4), 299–405. https://doi.org/10.1007/s11214-016-0282-z

Yamazaki, Y., Yumoto, K., Cardinal, M. G., Fraser, B. J., Hattori, P., Kakinami, Y., et al. (2011). An empirical model of the quiet daily geomagnetic field variation. *Journal of Geophysical Research*, *116*, A10312. https://doi.org/10.1029/2011JA016487